Transient Shear Response and Flow-Induced Microstructure of Isotropic and Nematic Rigid-Rod Poly(*p*-phenylenebenzobisthiazole) Solutions

Andrea W. Chow,* Richard D. Hamlin, and Caroline M. Ylitalo

Lockheed Palo Alto Research Laboratory, 0/93-50, B/204, Lockheed Missiles and Space Company, 3251 Hanover Street, Palo Alto, California 94304

Received June 3, 1992; Revised Manuscript Received August 24, 1992

ABSTRACT: Poly(*p*-phenylenebenzobisthiazole) (PBZT), a highly rigid-rod-like polymer that forms a lyotropic solution in strong acids such as methanesulfonic acid, was used as a model system to examine the transient flow properties and shear-induced microstructure near the isotropic–nematic phase transition. Upon flow reversal, two types of responses were observed in the nematic phase depending on the rod concentration and the applied shear rate. At low concentrations and low shear rates, the shear stress versus strain exhibits no overshoot, and the first normal stress transient is always positive. Such a response resembles those of the isotropic solutions. At higher concentrations and higher shear rates, damped oscillations in the shear stress and a negative transient followed by oscillatory behavior in the first normal stress were recorded. The material texture during flow and following flow cessation was examined using optical microscopy, and the macroscopic order parameter was measured using UV dichroism. The results indicate that the threshold shear rate dividing the flow response corresponds to the onset of shear-induced changes in the polydomain texture. This division is in agreement with the qualitative classification of regions I and III proposed by Onogi and Asada[1] for the flow behavior of liquid-crystalline polymers. The transient flow behavior of anisotropic PBZT solutions also depends on the solvent. In poly(phosphoric acid), the oscillations in shear stress upon flow reversal and step shear persist for a long time with very little damping in amplitude. Flow instability in a rotational viscometer at high shear rates was observed in both solvent systems.

Introduction

Solutions and melts of rodlike, liquid-crystalline polymers (LCP) have been known to exhibit flow properties dramatically different from those of their flexible counterparts due to molecular ordering in the liquid-crystalline state. Understanding of the complex rheological properties of lyotropic, nematic polymers is advancing steadily with recent progress in the experimental[1–14] as well as theoretical[15–27] investigations. On the basis of experimental observations, the steady shear viscosity of LCPs has been characterized into three regions depending on the shear rates:[1] region I shear thinning, region II Newtonian plateau, and region III shear thinning. Steady and transient shear flow properties in regions II and III have been studied quite extensively particularly for lyotropic poly(benzyl glutamate) (PBG). Reported transient flow phenomena include damped oscillations in shear stress scaled with strain following shear step-up and flow reversal,[5,6,8,11] and stress relaxation and strain recovery scaled with strain.[21,28] To our knowledge, no transient flow behavior in region I has been reported so far.

One of the most striking rheological properties exhibited by LCP is the negative first normal stress difference (N_1) under steady shear flow first reported by Kiss and Porter in 1978[2] on a study of PBLG solutions. The results were subsequently confirmed by others using other polymers including lyotropic (hydroxypropyl)cellulose (HPC),[12] and thermotropic polyesters.[29] Negative N_1 can be found near the transition from region II to region III. This phenomenon was unexplained for over a decade until Marrucci and Maffettone[19] provided a physical description based on their 2D analysis of the Doi molecular model.[15] Negative N_1 occurs when the degree of anisotropy under a shear field decreases below that of the quiescent state. Analyses of the Doi theory by Marrucci and Maffettone[23] and Larson[22] show that the sign change in the first normal stress difference during steady shear flows can be described qualitatively by Doi's molecular dynamics model without detailed knowledge on the domain structure. The transition from positive to negative N_1 occurs near the shear rate when the molecular dynamics change from director tumbling to wagging. Transient shear properties, on the other hand, are more sensitive to the microstructure in the nematic phase since a qualitative description of the observed transient shear behavior requires some phenomenological account of domainal dynamics in the model calculations.[27] Consequently, more experimental data on transient flows of LCPs are desirable to test the applicability of these phenomenological descriptions. Furthermore, the Doi model is capable of predicting regions II and III but not region I, possibly due to the fact that region I rheology is strongly influenced by the domain structure.[1] Thus, experimental data on the transient flow behavior in region I may also provide valuable insight into the domain structure and domain interactions.

In this paper, we present an experimental study of the transient flow properties and flow-induced microstructure of a highly rodlike polymer, poly(*p*-phenylenebenzobisthiazole) (PBZT), over a concentration range covering the isotropic–nematic phase transition. PBZT is an aromatic, heterocyclic rodlike polymer with a repeat unit structure:

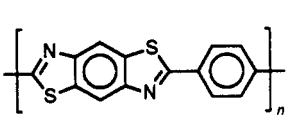

Its rigidity results from the 180° catenation angle (the angle between two exocyclic bonds) such that the overall conformation of the polymer is unaffected by the rotational isomeric states of the monomeric units. Dilute solution studies[30] confirm the rodlike conformation as indicated by the high Mark–Houwink exponent of 1.8 and a persistence length on the order of the molecular length.

As will be illustrated in this paper, the transient shear flow properties of PBZT in methanesulfonic acid (MSA)

* To whom correspondence should be addressed.

0024-9297/92/2225-7135$03.00/0

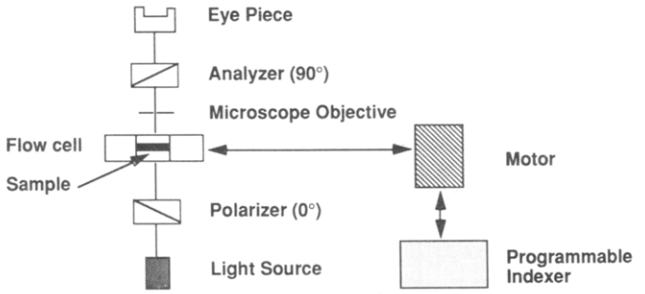

Figure 1. Schematic diagram of the experimental setup for the microscopy experiments.

are strongly dependent on the polymer concentration as well as the applied shear rate. In the nematic state, we have evidence of transient flow behavior in region I, which appears qualitatively different from that in regions II and III. The rheological results are complemented by order parameter measurements using ultraviolet (UV) dichroism and by direct observation under a polarized optical microscope in order to correlate liquid-crystalline texture with flow properties. We will also present rheological measurements of PBZT in its polymerization solvent poly(phosphoric acid) (PPA) and discuss some anomalous flow instabilities observed during rotational viscometric measurements.

Experimental Section

Material Preparation. All PBZT samples were provided in their polymerization solvent PPA as solution mixtures. For the studies in MSA, the polymer fraction was isolated from the PPA solution by precipitating in deionized water, and the residual PPA was thoroughly removed in a Soxhlet apparatus with water. The polymer was then dried in a vacuum oven at >130 °C for 24 h. The final solutions were prepared by dissolving dried PBZT in freshly distilled MSA at 60 °C for days to weeks and stored in a dry environment. Polymer concentrations ranging from 2.5% to 6.0% by weight were investigated. Using polarized optical microscopy and direct observations, the 2.5 wt % solution was found isotropic whereas the 3.8, 4.7, and 6.0 wt % ones were liquid crystalline. The polymer used in the MSA solutions has an intrinsic viscosity of 23.1 dL/g. Using the established Mark–Houwink relationship for PBZT,[30] the weight-average molecular weight is 33 500 Da. If 1.25 nm is assumed to be the length of a repeat monomer unit and 0.7 nm to be the molecular diameter,[31] the average length of a PBZT rod is calculated to be 158 nm with an aspect ratio of 225.

The PBZT/PPA samples used in the shear step-up experiments contained 4.5% and 15% by weight of PBZT, and the final P_2O_5 content in PPA was calculated to be 82.9%. For the 4.5 wt % solution, the intrinsic viscosity of the polymer is 8.76 dL/g. The weight-average molecular weight is 19 600 Da, with an average molecular length of 92 nm and an aspect ratio of 131. When examined under a polarized optical microscope equipped with a hot stage, this sample was determined to be liquid crystalline up to 200 °C. The intrinsic viscosity of the polymer in the nematic 15 wt % solution is 23.1 dL/g.

Rheological Measurements. A Rheometrics RMS-800 equipped with a 25-mm-diameter cone-and-plate fixture and 0.1-rad cone angle was used. In this geometry, the shear stress (σ_{12}, where 1 and 2 are the flow and shear gradient directions, respectively) and first normal stress difference ($N_1 = \sigma_{11}-\sigma_{22}$) are measured. In all experiments, dry nitrogen was used to purge the environmental chamber to avoid sample contamination by moisture. The temperature used for the PBZT/MSA solutions was 25 ± 1 °C. For the PBZT/PPA solutions, the experimental temperature ranged from 160 ± 1 to 200 ● 1 °C.

Polarized Optical Microscopy. The flow cell designed for microscopy studies consists of parallel fused silica windows (1-in. diameter) with an adjustable gap. A schematic diagram of the experimental step up is shown in Figure 1. A Teflon O-ring and vacuum grease were used to seal the polymer sample sandwiched between the windows in the flow cell from atmospheric moisture. The sample thickness was 100 μm. The lower window of the cell can be rotated to produce the desirable shear flow in the sample. The rotation speed was controlled by a programmable Compumotor indexer (model 4000) and a microstepping motor which is mechanically coupled to the flow cell. The polarizer and analyzer of the microscope were crossed at 90° in these experiments.

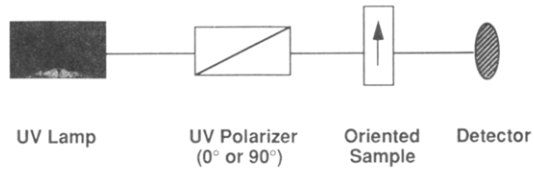

Figure 2. Optical train used for the UV dichroism experiments.

Ultraviolet (UV) Dichroism. UV dichroism is a spectroscopic technique that allows quantitative measurement of the mesoscopic order parameter of an anisotropic sample based on polarization-dependent UV absorption by the polymer chains. If the electric vector of the incident radiation is parallel to the transition dipole moment vector of the backbone, the absorption is maximum, whereas for orthogonal orientation, the absorption is minimum. On the other hand, UV absorption is independent of the polarization of the incident light in an isotropic sample. Using this technique, the order parameter, S, of a sample can be determined by[32,33]

$$S = \frac{(R-1)}{(R+2)}\frac{(R_0+2)}{(R_0-1)} \tag{1}$$

In this expression, R is the dichroic ratio defined by[32,33]

$$R = \frac{A_{par}}{A_{perp}} \tag{2}$$

A_{par} and A_{perp} are the areas under a given absorption peak measured with parallel and perpendicular polarized light with respect to the transition moment vector, respectively. R_0 in eq 1 depends on the angle (α) between the dipole moment vector and the molecular chain axis:

$$R_0 = 2\cot^2\alpha \tag{3}$$

For the selected absorption peak of PBZT at 269 nm, α equals 0° and eq 1 becomes

$$S = \frac{(R-1)}{(R+2)} \tag{4}$$

Figure 2 illustrates the optical train used for the UV dichroism measurements. The spectrophotometer is a Varian CARY 219. The experiments were conducted using the same flow cell and motor control described above. In this geometry, anisotropy in the flow-vorticity plane ($S_{11} - S_{33}$, where 3 is the vorticity direction) is measured. The shear rates were calculated at a point $^3/_8$ in. away from the center of the window. A narrow slit $^1/_{16}$ in. wide and $^1/_4$ in. long, positioned at $^3/_8$ in. tangentially along the radial direction from the cell center, was used to define the position and sampling area for the UV measurements. The streamlines framed by the slit were assumed to be approximately straight lines. The fused silica windows, with a cutoff absorption of 220 nm, do not absorb UV radiation at the wavelength range of interest. The polarizer is made of quartz with a cutoff absorption around 240 nm. The solvent MSA is found to be transparent in the entire UV region considered. Absorption of UV light by the polymer, however, is very high. Thus, the experiments were limited to very thin samples of 43 μm.

Results and Discussion

Due to the multiphasic nature of LCPs, the microstructure and hence rheological properties can be strongly dependent on the shear and temperature histories experienced by the materials. Furthermore, PBZT is known to have long relaxation times[14] such that removing the shear effects resulting from sample loading could be impractical. As a result, all transient flow experiments conducted in this study consisted of some preshearing of the sample to yield a well-defined initial condition. These

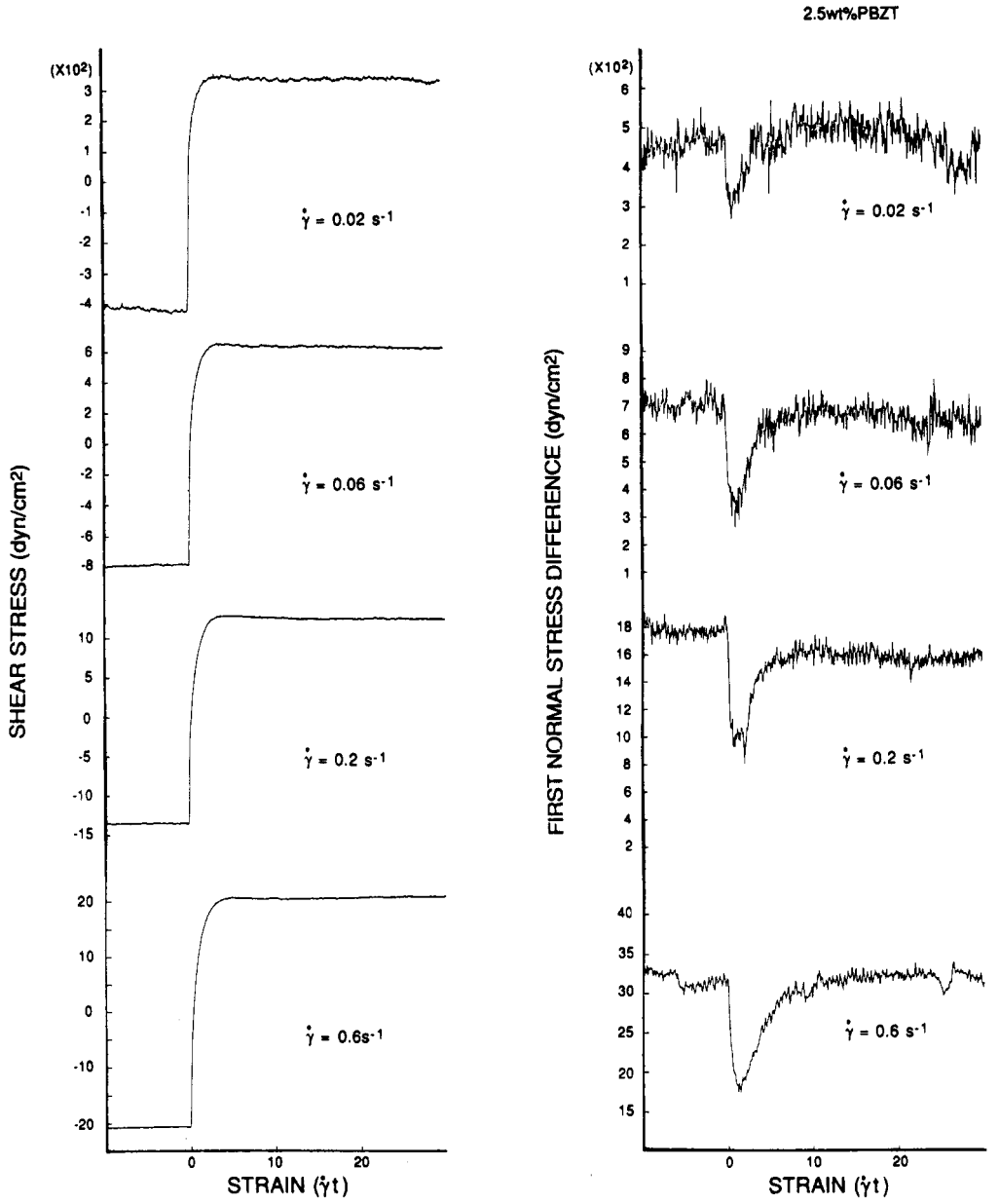

Figure 3. Shear stress and first normal stress difference as a function of strain for the 2.5 wt % PBZT/MSA solution upon flow reversal at various shear rates ($\dot{\gamma}$). Reversal of the applied shear occurs at strain 0.

transient flows include flow reversal and step-up of shear. The shear rate range reported in the following section is limited by the transducer sensitivity at the low end and secondary flows occurring at the high end. Flow instability resulting from secondary flows will be discussed separately in a later section.

PBZT/MSA: Shear and Normal Stress. Figure 3 illustrates the flow reversal response of the isotropic, 2.5 wt % PBZT/MSA solution for a range of shear rates. The shear stress and the first normal stress difference are plotted as a function of strain units at several shear rates ($\dot{\gamma}$). Upon flow reversal (at strain 0), the shear stress changes sign and reaches its steady-state value monotonically without any noticeable stress overshoot. N_1, on the other hand, shows a dip during flow reversal and recovers back to its steady-state value in less than 10 strain units. Note that the minimum in N_1 is always greater than zero.

For the most concentrated, anisotropic PBZT/MSA solution of 6.0 wt %, the response during flow reversal, as shown in Figure 4, is markedly different qualitatively. The shear stress exhibits a significant overshoot and a very small undershoot (appearing to be highly damped oscillations) before reaching the steady-state value. N_1 exhibits oscillatory behavior even after large strain (over 200 units), and the minimum transient N_1 value immediately following flow reversal is always *negative*.

The flow reversal behaviors of the two intermediate concentrations, 3.8 and 4.7 wt % solutions, are illustrated in Figures 5 and 6, respectively. For the 3.8 wt % solution, which is liquid crystalline, both the shear and normal stresses are reminiscent of those characteristic of the isotropic solution (2.5 wt %, see Figure 3). The shear stress shows no observable overshoot, whereas N_1 possesses a transient minimum that is always *positive* in value. For the 4.7 wt % solution (Figure 6), the stresses following flow reversal mimic those of the 3.8 wt % mixture at shear rates up to 0.35 s^{-1} but begin to resemble the response of the 6.0 wt % mixture at higher shear rates. These results appear confusing initially because the two types of characteristic behavior do not correspond solely to the isotropic and nematic phases. In the nematic phase, the response to flow reversal is a function of the concentration as well as the applied shear rate.

When the steady-state values of the stresses are plotted as a function of shear rate, a plausible explanation for the transient flow behavior in the nematic phase begins to emerge. Figure 7 illustrates the shear viscosity calculated from the steady values of the shear stress versus shear

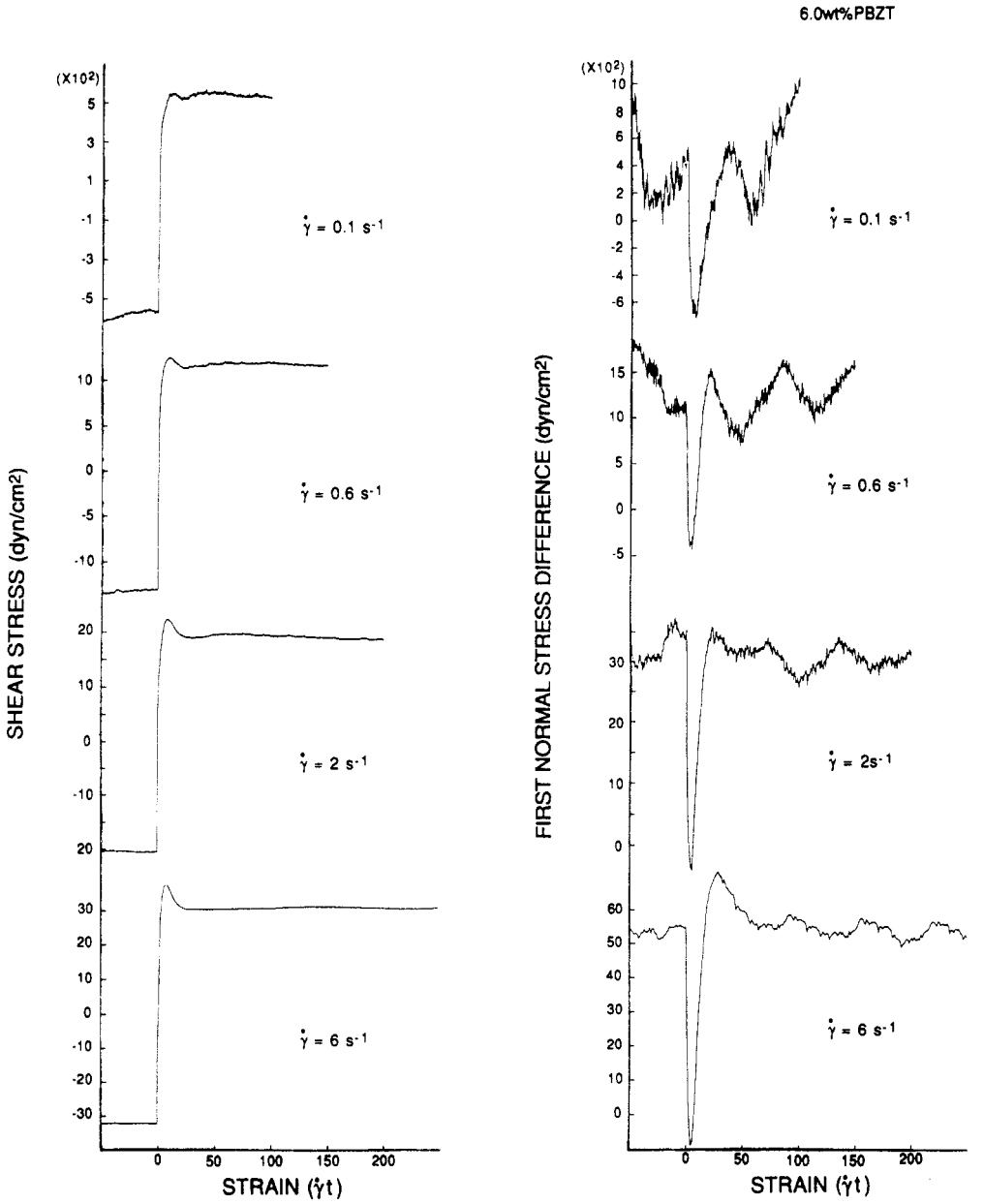

Figure 4. Shear stress and first normal stress difference as a function of strain for the 6.0 wt % PBZT/MSA solution upon flow reversal at various shear rates ($\dot{\gamma}$). Reversal of the applied shear occurs at strain 0.

rate. All concentrations exhibit shear-thinning behavior. However, for the 4.7 wt % solution, a break in slope in the shear-thinning curve appears near 0.35 s^{-1}, the shear rate at which the flow reversal response changes from one characteristic behavior to another as described above. Such a break in the slope in the shear viscosity has also been observed by Einaga et al. in PBZT/MSA samples.[4] Using Onogi and Asada's description, the region below 0.35 s^{-1} may be classified as region I shear thinning and that above 0.35 s^{-1} as region III shear thinning. The region II Newtonian plateau is not discernible in this sample as has been observed in a number of other liquid-crystalline polymers.[34]

The framework proposed by Onogi and Asada[1] appears to be helpful in understanding the rheological response of the PBZT/MSA nematic solutions. In Region I, which includes the 3.8% sample in the entire shear rate range studied and the 4.7% sample up to 0.35 s^{-1}, the flow properties may be dominated by the polydomain structure, resulting in one type of flow response. In region III, which encompasses the 4.7% sample at shear rates above 0.35 s^{-1} and the 6.0% sample in the entire shear rate range examined, the flow properties may be dominated by the shear field as the material microstructure is modified by the flow, resulting in a different type of response. This tentative explanation of the two different flow responses is based on some qualitative description of the liquid-crystalline microstructure during flow. To lend support to this explanation, we examined the PBZT/MSA samples under a polarized optical microscope during shear and characterized the macroscopic flow-induced orientation at steady state using UV dichroism. The microstructure results are presented in the following section.

Incidentally, under the experimental conditions chosen, we did not observe a negative N_1 at steady state for any of the nematic PBZT/MSA samples. Figure 8 is a summary plot showing steady-state values of N_1 as a function of shear rate for all four concentrations. In cases where N_1 values exhibit periodic behavior even after large strain, an average of the magnitude of the oscillation was taken as the "steady-state" value. The periodic oscillations in N_1 may be a manifestation of director tumbling.

PBZT/MSA: Microstructure Characterization. Under crossed polarizers of the optical microscope, the isotropic 2.5 wt % solution appears dark and featureless at rest. When sheared, the sample becomes birefringent with red, orange, yellow, and green concentric rings appearing at the outer edges of the windows first and

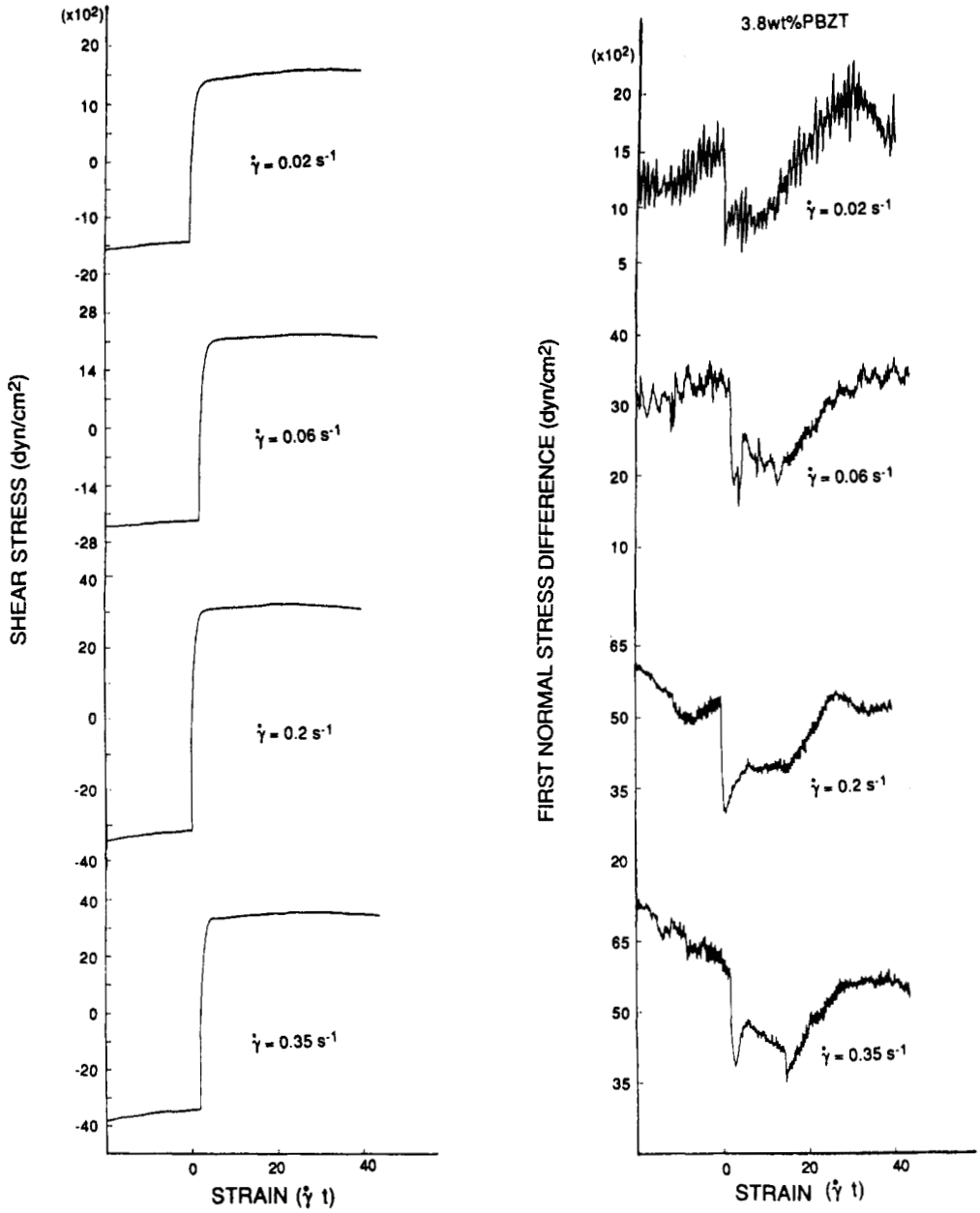

Figure 5. Shear stress and first normal stress difference as a function of strain for the 3.8 wt % PBZT/MSA solution upon flow reversal at various shear rates ($\dot{\gamma}$). Reversal of the applied shear occurs at strain 0.

moving toward the center of the flow cell with time at constant applied shear until the steady state is reached. This concentric-ring pattern is due to the radially varying shear rate of the parallel disk geometry, resulting in an increasing degree of flow-induced anisotropy radially outward. Upon cessation of flow, the birefringence disappears within a few tens of seconds. The time scale for the birefringence relaxation is comparable to those of stress relaxation as illustrated in Figure 9.

When viewed under the microscope between crossed polarizers, the anisotropic solutions (3.8, 4.7, and 6.0 wt %) after sample loading are strongly birefringent with a pronounced texture in the form of yellow, green, orange, and red "regions" of random orientation. These "regions" are of the order of 1–10 μm, with a smaller characteristic length scale at higher PBZT concentration in general. Figure 10a is an optical micrograph of the 6.0 wt % solution at rest. Notice that around the edges the domains are oriented radially, most likely resulting from sample loading when the solution is squeezed outward between the optical windows. These loading effects persist for several hours.

When the nematic solutions were sheared, the following general features were observed. At very low shear rates the texture of the nematic solutions looks unperturbed from the rest state. As the shear rate increases, the colored regions elongate to become elliptical in shape and start to align along the streamlines. Eventually, at even higher shear rates, the colored texture disappears, yielding a uniform color in the entire field of view while a Maltese cross centered at the rotational center of the flow cell appears. The dark arms of the cross are always oriented parallel to the optical axis of the two crossed polarizers. This orientation is clearly seen in Figure 10b for the 6.0 wt % solution. Notice that near the center of the cross where the shear rate is lowest, one can see the yellow regions oriented along the streamlines. Also evident in this figure is the texture refinement with shear when compared with Figure 10a. The phenomenon that the texture becomes finer with increasing shear rate has been predicted by theory[27] and observed experimentally in thermotropic LCPs[35] and in lyotropic PBLG.[28] The Maltese cross remains clearly visible for several hours after shear cessation.

Upon flow reversal no significant changes in the solution texture are seen. The regions seem to rearrange immediately after flow reversal (within 1 s), and then the general

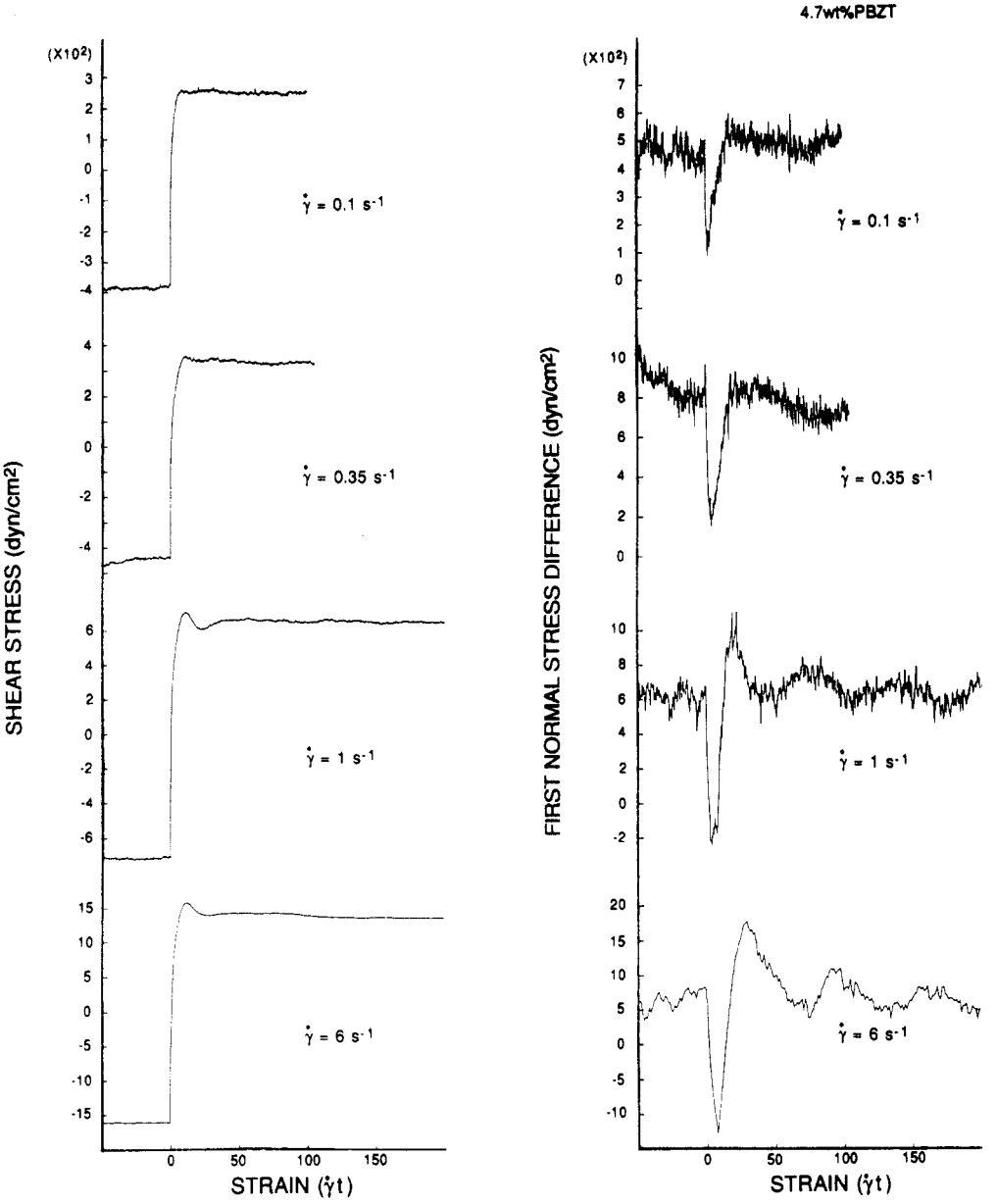

Figure 6. Shear stress and first normal stress difference as a function of strain for the 4.7 wt % PBZT/MSA solution upon flow reversal at various shear rates ($\dot{\gamma}$). Reversal of the applied shear occurs at strain 0.

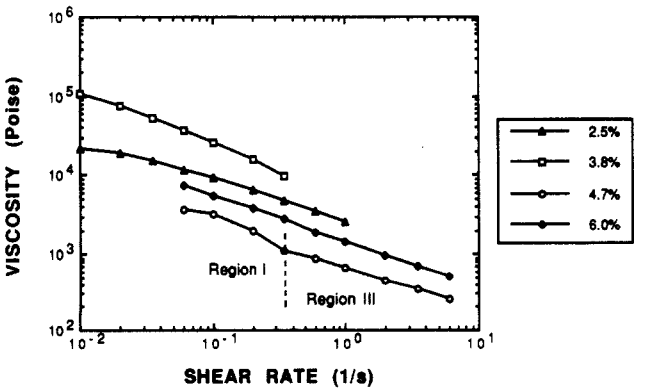

Figure 7. Steady shear viscosity as a function of the applied shear rate for PBZT/MSA solutions at four different polymer concentrations.

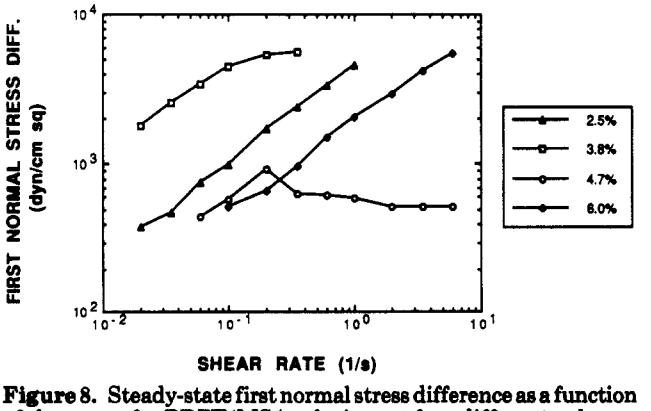

Figure 8. Steady-state first normal stress difference as a function of shear rate for PBZT/MSA solutions at four different polymer concentrations.

features become similar to those observed before the reversal of the flow.

When the flow is stopped, the texture does not exhibit noticeable change for several hours, indicating that texture relaxation is a very slow process in nematic PBZT. Eventually, the Maltese cross disappears and the texture becomes coarser with time until it resembles the presheared solution texture. This texture relaxation time is found to be a function of solution concentration as well as shear rate, and it is found to vary between 8 and 14 h. Stress relaxation, on the other hand, is much faster and usually achieved within a few tens of seconds as evident in Figure 11. The existence of two relaxation times, namely, a fast

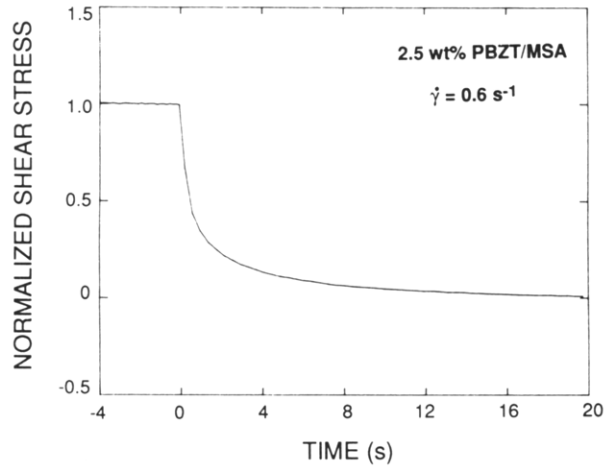

Figure 9. Stress relaxation for the isotropic, 2.5 wt % PBZT/MSA solution. The applied shear ($\dot{\gamma}$ = 0.6 s^{-1}) stops at time 0.

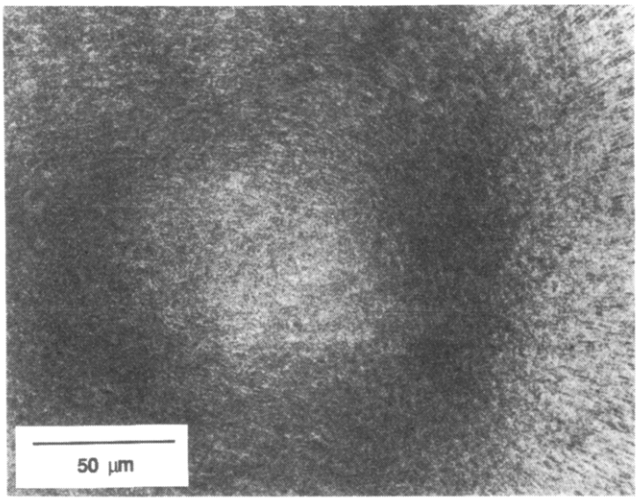

(a)

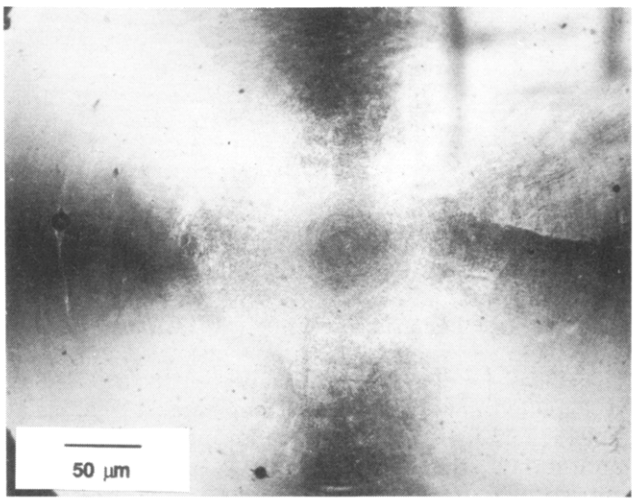

(b)

Figure 10. Optical micrographs for the 6.0 wt % PBZT/MSA solution: (a) sample at rest after loading, (b) appearance of Maltese cross when the sample is sheared.

stress relaxation and a slow texture relaxation, is consistent with several other observations in the literature.[5,36]

Quantitative descriptions of the observed flow-induced microstructural changes have been obtained using UV dichroism to measure the mesoscopic order parameter, S.

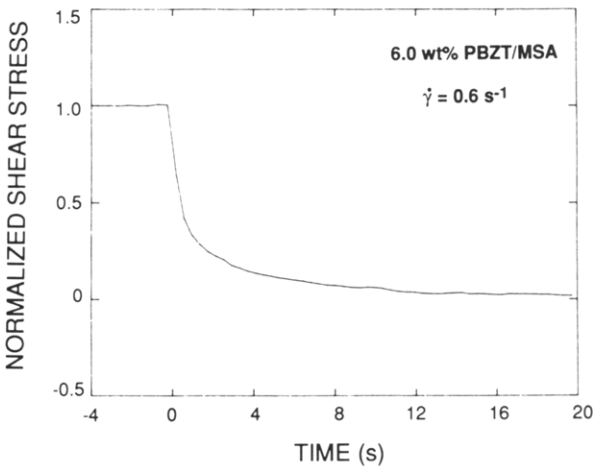

Figure 11. Stress relaxation for the anisotropic, 6.0 wt % PBZT/MSA solution. The applied shear ($\dot{\gamma}$ = 0.6 s^{-1}) stops at time 0.

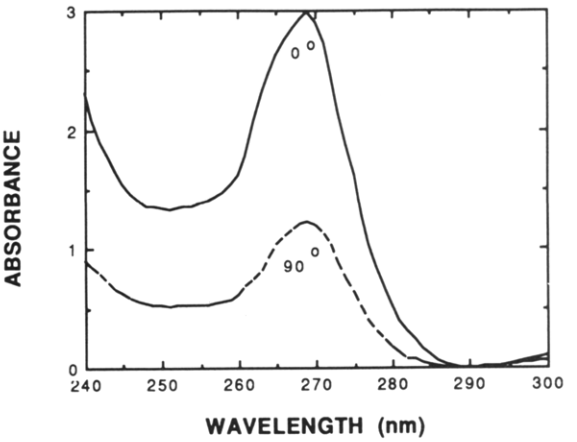

Figure 12. Polarized UV spectra for the 4.6 wt % PBZT/MSA solution after shearing at 6 s^{-1}.

The sample was placed in the spectrophotometer after shearing, and two spectra were measured: one with the polarizer at 0° with respect to the flow direction and the other at 90°. These spectra were acquired within 20 min of flow cessation. Since texture relaxation of the nematic solutions occurs over a period of several hours for these solutions, we assume that the order parameter measured from these experiments is the same as that during shear. Figure 12 shows the two polarized spectra for the 4.7 wt % solution. The areas under the 269-nm peaks were used to calculate the order parameter as described in the Experimental Section.

The measured order parameters for the PBZT solutions as a function of shear rate are shown in Figure 13. As expected, the 2.5 wt % isotropic solution has a zero-order parameter within experimental error at all shear rates since relaxation of the flow-induced order is faster than the time required to take the UV spectra. The 3.8 wt % nematic solution also yields zero values of S at shear rate as high as 5 s^{-1}, suggesting that the random distribution of the ordered regions has not been altered by flow. The value of S for the 4.7 wt % solution remains zero up to a shear rate of 0.8 s^{-1}, and then it increases linearly with the logarithm of the shear rate. Finally, the 6.0 wt % solution gives a finite and measurable order parameter at the lowest shear rate examined. Again S increases linearly with the logarithm of the shear rate until 2.0 s^{-1}, beyond which the sensitivity of the spectrophotometer is saturated for this sample.

Comparison of Rheology and Microstructure. The optical microscopy and UV dichroism results support

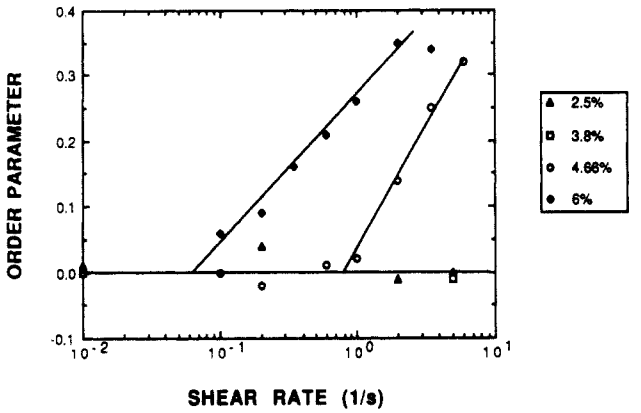

Figure 13. Order parameter as a function of the applied shear rate for PBZT/MSA solutions at four different polymer concentrations.

Onogi and Asada's proposed shear-induced microstructure of LCPs in regions I and III. It is most evident when the rheological measurements of the 4.7 wt % PBZT/MSA solution, which exhibit two types of transient flow behavior, are compared with the microstructure results. For this nematic solution, two characteristic types of texture were observed under the microscope depending on the shear rate. At low shear the polydomain structure was not perturbed by the applied flow field. At high shear the polydomain structure was destroyed while the polymer rods were aligned in the flow direction as suggested by the disappearance of the multicolor regions and the appearance of the Maltese cross. The Maltese cross occurs under crossed polarizers because the molecules align along the flow direction such that the principal optical axis of the sample is parallel to one of the polarizers of the microscope, resulting in no light transmission. When the sample is rotated, the cross remains stationary, indicating that the orientation of the rigid rods is equivalent in all radial directions as expected. On the other hand, when one polarizer is rotated, one arm of the Maltese cross rotates with it. These observations are further supported by the order parameter measurements which give two types of values: zero below a threshold shear rate and nonzero above. Thus, qualitatively, the transient flow properties measured for PBZT/MSA mixtures can be nicely correlated with the domain structure observed for these solutions.

Quantitatively, comparison of the threshold shear rate dividing the low shear (region I) and high shear (region III) behavior determined from rheological and microstructural measurements (0.35 and 0.8 s^{-1}, respectively) is only fair. This discrepancy is unlikely to be due to errors in determining the shear rate because the microstepping motor control used to control the optical flow cell should be quite precise. We believe that the disagreement could result from the difference in flow geometries (cone-and-plate for the rheometric and parallel plates for the UV dichroism measurements) and the sample thickness since surface effects are notoriously influential in liquid-crystalline materials. Moreover, the measured order parameters may be artifically lower than the true values, possibly leading to a slight overestimate of the threshold shear rate. The error in determining the order parameter may be due to several factors including the time lag between flow cessation and UV absorbance measurements, partial depolarization of the UV beam as it travels through the thick flow cell windows ($^1/_4$ in. thick), and the curved streamlines of the flow cells. All of these factors could reduce the magnitude of the order parameter slightly but should not affect the overall trends and thus our conclusions deduced from these results.

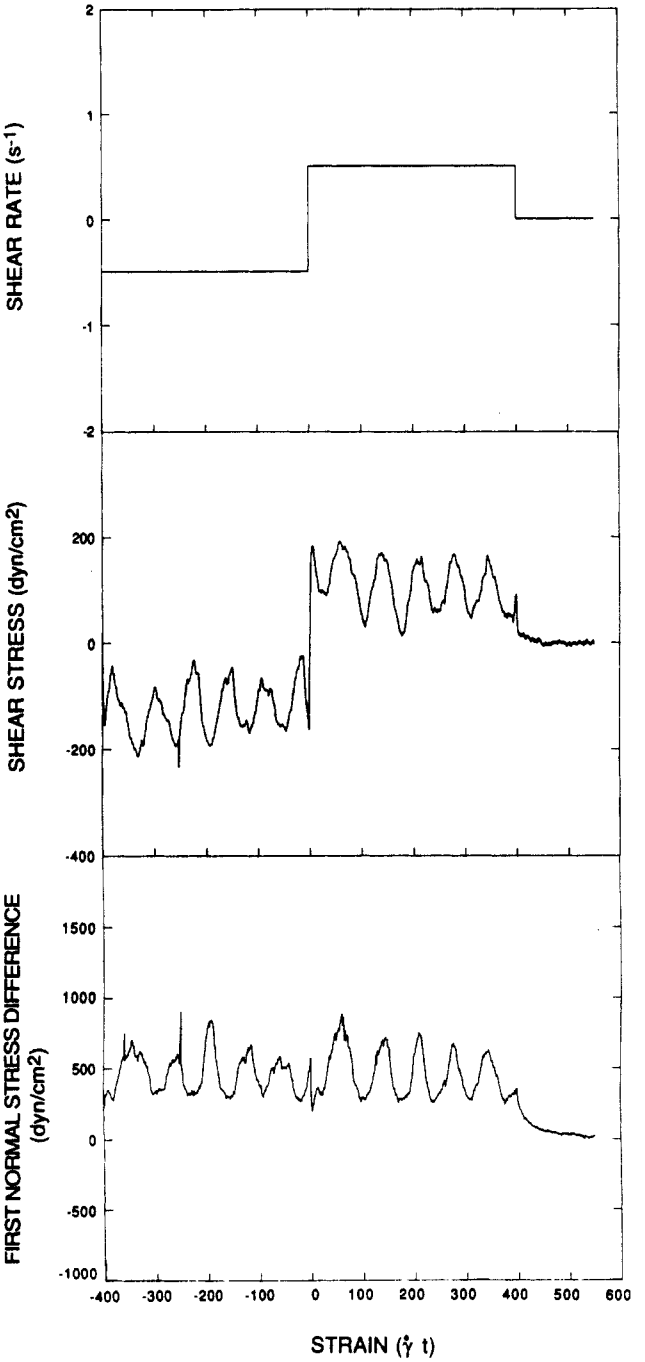

Figure 14. Transient response of the 15 wt % PBZT/PPA solution following reversal of shear at 0.5 s^{-1}.

In summary, our data indicate that transient flow measurements and microstructural characterization of isotropic and nematic solutions of PBZT/MSA are well correlated. For nematic solutions at low shear rate, the so-called region I in the classification of Onogi and Asada, the applied flow field is not strong enough to affect the polydomain structure of the solution. The transient shear and normal stresses upon flow reversal exhibit characteristic behavior different from those observed in region II (PBG) and region III (PBG and PBZT). It is interesting that the flow dynamics measured in region I resemble those observed in the isotropic solution.

Our investigation combining rheological measurements with microstructural studies provides some information on the flow response in region I, a region that has not been examined extensively in the past. However, our data do not shed light on the detailed mechanisms by which the polydomain texture resists flow-induced changes in region I. The resistance may be due to elastic forces resulting from surface effects or interactions between domains.

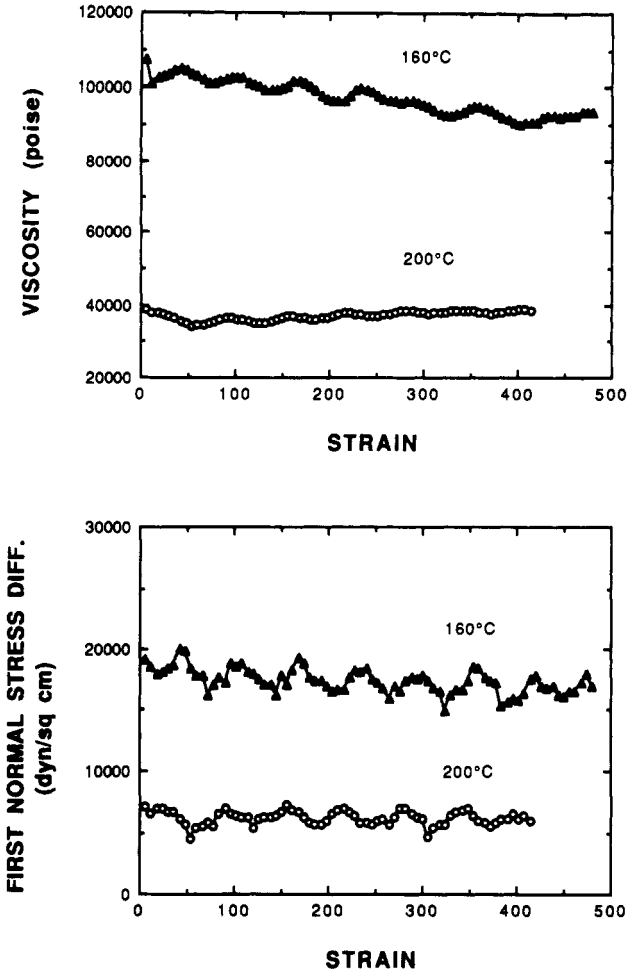

Figure 15. Shear viscosity and first normal stress difference for the 4.5 wt % PBZT/PPA solution as a function of strain following shear step-up from 0.01 to 0.1 s^{-1}.

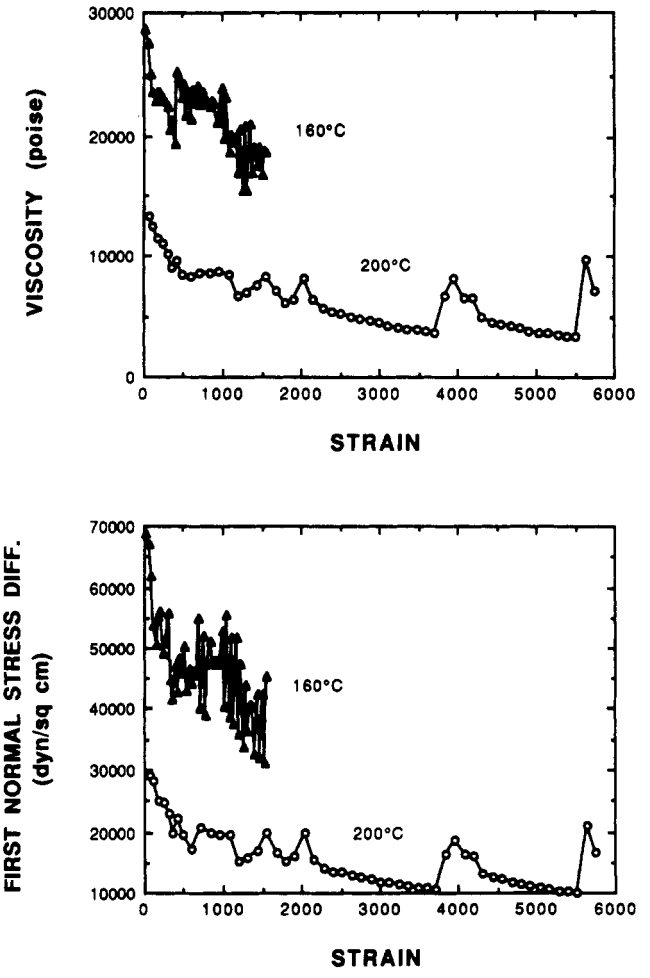

Figure 16. Shear viscosity and first normal stress difference for the 4.5 wt % PBZT/PPA solution as a function of strain following shear step-up from 0.1 to 1.0 s^{-1}.

During shear and upon cessation of shear flow for several LCPs, a number of researchers have reported the formation of dark and light bands perpendicular to the shear direction.[14,37-41] The appearance of this banded structure has been attributed to texture relaxation.[38] In our experiments, we did not observe this phenomenon during flow or relaxation even after a period of several hours.

PBZT/PPA: Shear and Normal Stresses. One of our motivations in studying the transient shear response of anisotropic PBZT/PPA solutions comes from our earlier observation that flow instability occurred at high shear rates (>5 s^{-1}) in the liquid-crystalline state when the rheological behavior of PBZT polymerization in PPA was investigated.[31] In this study, we examined samples that had been end-capped so that the complexity of changing molecular weight is eliminated.

Figure 14 illustrates the transient stresses of the 15 wt % PBZT/PPA solution at 180 °C upon reversal of shear. As shown in the top curve, at strain 0, the shear rate of 0.5 s^{-1} was reversed in direction and then stopped after 400 strain units. Unlike the response of the PBZT/MSA samples, the shear stress (middle curve) exhibits somewhat periodic fluctuations with very little damping in magnitude. The first normal stress difference (lower curve) also shows periodic oscillations, and the transient immediately following flow reversal is positive.

Two temperatures, 160 and 200 °C, were selected to examine the step shear response of the 4.5 wt % PBZT/PPA solution since this range of temperatures is of interest for processing. At each temperature, the solution was first subjected to a steady shear of 0.01 s^{-1} for 180 min (strain 108) to remove any shear histories resulting from sample loading. The shear rate was then stepped to 0.1 s^{-1}, the corresponding transient was more or less constant, and the damping of the periodic oscillation was very small. We did not measure such periodic fluctuations for melts of flexible polymers with comparable shear stress levels, thereby eliminating the possibility that the oscillations may be due to instrument artifacts. This behavior is qualitatively different from those found in the PBZT/MSA nematic systems which exhibit highly damped oscillations in shear stresses upon step shear. Such a difference may be attributed to the solvent effects and is a topic for future studies. Recently, Ernst and Denn[42] reported no oscillations during startup of steady shear for poly(*p*-phenylenebenzobisoxazole) (PBO) in PPA, a system akin to PBZT in PPA. On the basis of the viscosity–shear rate curves of the PBO/PPA systems examined by these researchers, the shear rate range at which the startup experiments were performed appeared to fall in region I.

When the shear rate was further stepped up to 1.0 s^{-1} from 0.1 s^{-1}, some aperiodic fluctuations in the shear and normal stresses can be observed as illustrated in Figure 16. We believe that this behavior may be a manifestation of the onset of secondary flows related to our earlier observation in polymerizing PBZT in PPA. As mentioned earlier, we also observed rotational flow instability in the PBZT/MSA mixtures.

Flow Instability. When we pulled the cone-and-plate flow cell apart after aperiodic fluctuations in the stress signals were observed, we found evidence of secondary flows throughout the flow cell. Material started to organize itself concentrically around the center of the cell. Under prolonged shear, a "bullseye" can in fact be seen on the

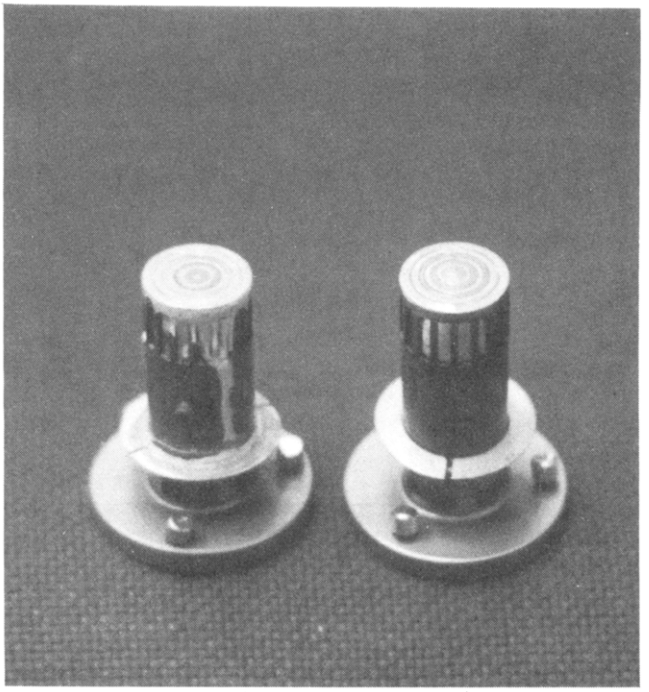

Figure 17. Rotational flow instability which appears as a bullseye pattern on the separated cell exhibited by the anisotropic 4.7 wt % PBZT/MSA solution after prolonged shearing at high shear rates in the cone-and-plate flow cell.

separated flow cell surfaces. Figure 17 is a photograph of the separated cone-and-plate flow cell after the anisotropic, 4.7 wt % PBZT/MSA mixture has been sheared at 5 s^{-1} for 900 strain units. The flow cell was submerged in water immediately after being removed from the rheometer in order to preserve the structure. Formation of such an unusual pattern was observed in both the anisotropic PBZT/PPA solutions and the nematic solutions of PBZT/MSA. Our results indicated that the concentric-ring pattern was associated with the liquid-crystalline phases and not observed in the 2.5 wt % isotropic of PBZT in MSA. Similar flow instabilities have been reported in the literature for a thermotropic LCP.[43] In that case, the concentric-ring pattern has been attributed to bubbles produced by polymer offgassing. These bubbles were aligned under shear and coalesced into concentric rings. In our system, it is doubtful that the mechanism leading to such an unusual pattern is similar, although it is conceivable that bubbles could form as the acids interact with the stainless steel rheometer fixture. The solutions themselves should be chemically stable at the temperatures used in this study. The PBZT chains were end-capped to eliminate further polymerization upon heating, and there was no physical evidence (color change, for example) to indicate chemical or physical changes due to moisture absorption.

Conclusions

In this study, we found that the transient flow response of PBZT in the anisotropic phase and its flow-induced texture are intimately interrelated. Within the ranges of concentration and shear rate examined for the PBZT/MSA solutions, we identified the piled polydomain region I and flow-oriented region III. Transient flow behaviors upon reversal of shear have been obtained in these regions. As a model system for studying the dynamics of LCP, PBZT exhibits some shear responses different from those of other model systems such as PBG. Moreover, the response of anisotropic PBZT mixtures appears to depend strongly on the rod concentration, shear rate, and solvent used. These observations point to the need for more experimental studies on a larger set of LCP systems to assist the development of a unified molecular theory describing the dynamics of LCPs.

Acknowledgment. This research was funded by the Lockheed Independent Research program. We gratefully acknowledge Dr. James Wolfe for providing the PBZT samples and the intrinsic viscosity data, and for many useful discussions throughout the course of this study. We also would like to thank Dr. Ronald Larson for the helpful discussion on data interpretation, and Drs. Jerry McCauley and Volker Abetz for their assistance in the UV dichroism measurements.

References and Notes

(1) Onogi, S.; Asada, T. In *Rheology*; Astarita, G., Marrucci, G., Nicolais, L., Eds.; Plenum Press: New York, 1980.
(2) Kiss, G.; Porter, R. S. *J. Polym. Sci., Polym. Symp.* **1978**, *65*, 193.
(3) Kiss, G.; Porter, R. S. *J. Polym. Sci., Polym. Phys. Ed.* **1980**, *18*, 361.
(4) Einaga, Y.; Berry, G. C.; Chu, S. G. *Polym. J.* **1985**, *17*, 239.
(5) Moldenaers, P.; Mewis, J. *J. Rheol.* **1986**, *30*, 567.
(6) Mewis, J.; Moldenaers, P. *Mol. Cryst. Liq. Cryst.* **1987**, *153*, 291.
(7) Mewis, J.; Moldenaers, P. *Chem. Eng. Commun.* **1987**, *53*, 33.
(8) Moldenaers, P.; Mewis, J. *Proc. Int. Congr. Rheol., 10th* **1988**, *2*, 134.
(9) Berry, G. C. *Mol. Cryst. Liq. Cryst.* **1988**, *165*, 333.
(10) Berry, G. C.; Se, K.; Srinivasarao, M. In *High Modulus Polymers*; Zachariades, A. E., Porter, R. S., Eds.; Dekker: New York, 1988.
(11) Moldenaers, P.; Fuller, G.; Mewis, J. *Macromolecules* **1989**, *22*, 960.
(12) Grizzuti, N.; Cavella, S.; Cicarelli, P. *J. Rheol.* **1990**, *34*, 1293.
(13) Burghardt, W. R.; Fuller, G. G. *Macromolecules* **1991**, *24*, 2546.
(14) Srinivasarao, M.; Berry, G. C. *J. Rheol.* **1991**, *35*, 379.
(15) Doi, M. *J. Polym. Sci., Polym. Phys. Ed.* **1981**, *19*, 229.
(16) Marrucci, G. *Mol. Cryst. Liq. Cryst.* **1982**, *72*, 153.
(17) Kuzuu, N.; Doi, M. *J. Phys. Soc. Jpn.* **1983**, *52*, 3486.
(18) Kuzuu, N.; Doi, M. *J. Phys. Soc. Jpn.* **1984**, *53*, 1031.
(19) Marrucci, G.; Maffettone, P. L. *Macromolecules* **1989**, *22*, 4076.
(20) Larson, R. G.; Mead, D. W. *J. Rheol.* **1989**, *33*, 185.
(21) Larson, R. G.; Mead, D. W. *J. Rheol.* **1989**, *33*, 1251.
(22) Larson, R. G. *Macromolecules* **1990**, *23*, 3983.
(23) Marrucci, G.; Maffettone, P. L. *J. Rheol.* **1990**, *34*, 1217.
(24) Cocchini, F.; Aratari, C.; Marrucci, G. *Macromolecules* **1990**, *23*, 4446.
(25) Magda, J. J.; Baek, S. G.; K, L. D.; Larson, R. G. *Macromolecules* **1991**, *24*, 4460.
(26) Marrucci, G. *Macromolecules* **1991** *24*, 4176.
(27) Larson, R. G.; Doi, M. *J. Rheol.* **1991**, *35*, 539.
(28) Burghardt, W. R.; Fuller, G. G. *J. Rheol.* **1990**, *34*, 959.
(29) Gotsis, A. D.; Baird, D. G. *Rheol. Acta* **1986**, *25*, 2275.
(30) Berry, G. C.; Metzger, P. C.; Venkatraman, S.; Cotts, D. B. *Polym. Prepr. (Am. Chem. Soc., Div. Polym. Chem.)* **1979**, *20*, 42.
(31) Chow, A. W.; Sandell, J. F.; Wolfe, J. F. *Polymer* **1987**, *29*, 1307.
(32) Tassin, J. F.; Monnerie, L.; Fetters, L. J. *Polym. Bull.* **1986**, *15*, 165.
(33) Tassin, J. F.; Monnerie, L.; Fetters, L. J. *Macromolecules* **1988**, *21*, 2404.
(34) Wissbrun, K. F. *J. Rheol.* **1981**, *25*, 619.
(35) Alderman, N. J.; Mackley, M. R. *Faraday Discuss. Chem. Soc.* **1985**, *79*, 1.
(36) Onogi, Y.; White, J. L.; Fellers, J. F. *J. Non-Newtonian Fluid Mech.* **1980**, *7*, 121.
(37) Viney, C.; Donald, A. M.; Windle, A. H. *Polymer* **1985**, *26*, 870.
(38) Navard, P. *J. Polym. Sci., Polym. Phys. Ed.* **1986**, *24*, 435.
(39) Marrucci, G.; Grizzuti, N.; Buonaurio, A. *Mol. Cryst. Liq. Cryst.* **1987**, *153*, 263.
(40) Doppert, H. L.; Picken, S. J. *Mol. Cryst. Liq. Cryst.* **1987**, *153*, 109.
(41) Ernst, B.; Navard, P. *Macromolecules* **1989**, *22*, 1419.
(42) Ernst, B.; Denn, M. M. *J. Rheol.* **1992**, *36*, 289.
(43) Kalika, D. S.; Giles, D. W.; Denn, M. M. *J. Rheol.* **1990**, *34*, 139.

Registry No. PBZT, 69794-31-6; MSA, 75-75-2.